Simple plasma assisted atomic layer deposition technique for high substitutional nitrogen doping of TiO_2

Abdullah H. Alshehri, Nathan Nelson-Fitzpatrick, Khaled H. Ibrahim, Kissan Mistry, Mustafa Yavuz, and Kevin P. Musselman

Citation: Journal of Vacuum Science & Technology A **36**, 031602 (2018); doi: 10.1116/1.5019170
View online: https://doi.org/10.1116/1.5019170
View Table of Contents: http://avs.scitation.org/toc/jva/36/3
Published by the American Vacuum Society

Simple plasma assisted atomic layer deposition technique for high substitutional nitrogen doping of TiO_2

Abdullah H. Alshehri
Department of Mechanical and Mechatronics Engineering, University of Waterloo, 200 University Ave. West, Waterloo, Ontario N2L 3G1, Canada and Department of Mechanical Engineering, Prince Sattam bin Abdul Aziz University, Alkharj 11942, Saudi Arabia

Nathan Nelson-Fitzpatrick
Quantum NanoFab, University of Waterloo, 200 University Ave. West, Waterloo, Ontario N2L 3G1, Canada

Khaled H. Ibrahim, Kissan Mistry, Mustafa Yavuz, and Kevin P. Musselman[a)]
Department of Mechanical and Mechatronics Engineering, University of Waterloo, 200 University Ave. West, Waterloo, Ontario N2L 3G1, Canada and Waterloo Institute for Nanotechnology, University of Waterloo, 200 University Ave. West, Waterloo, Ontario N2L 3G1, Canada

(Received 11 December 2017; accepted 26 February 2018; published 21 March 2018)

In this work, a plasma assisted atomic layer deposition system was used to deposit nitrogen-doped titanium dioxide. A simple approach was developed that requires only a nitrogen plasma and short plasma exposure times to effectively dope TiO_2. A range of nitrogen concentrations were achieved by varying the flow rate and exposure times of nitrogen and oxygen plasmas. A nitrogen content as high as 23 ± 0.5 at. % was observed when only the nitrogen plasma was used. It was also possible to vary the type of nitrogen doping from almost entirely interstitial to purely substitutional, as measured by x-ray photoelectron spectroscopy. Ultraviolet-visible spectroscopy measurements showed a shifting in the absorption edge from 350 to 520 nm with doping, indicating bandgap narrowing from 3.1 to 1.9 eV. *Published by the AVS.* https://doi.org/10.1116/1.5019170

I. INTRODUCTION

Titanium dioxide (TiO_2) has been used for a variety of applications including sensors,[1] photovoltaics,[2] and photocatalysis for environmental and energy purposes (e.g., self-cleaning surfaces and water and air purification)[3,4] because it is chemically stable, cheap, abundant, and nontoxic. However, the large bandgap of the anatase form of TiO_2 (3.1 eV) limits the efficiency of photocatalysis under visible light, and the position of its conduction band influences electron transport in devices such as photovoltaics and metal-insulator-metal diodes. To enhance the photocatalytic efficiency of TiO_2 and improve the current–voltage characteristics of TiO_2 devices,[5] nitrogen doping (N-doping) has been used to narrow the bandgap and increase visible light absorption. Various deposition processes have been used to introduce nitrogen atoms into the TiO_2 lattice of nanoscale films. These have included sputtering,[6] chemical vapor deposition,[7] and atomic layer deposition (ALD).[8] ALD has been used to deposit TiO_2 thin films using water vapor and a variety of different precursors as the Ti source, including titanium tetrachloride ($TiCl_4$),[9] titanium tetrafluoride (TiF_4),[10] tetrakis (dimethylamino)-titanium (TDMAT),[11] and titanium isopropoxide (TIIP).[12,13] Much research on N-doping with ALD has used NH_3 gas or ammonia water.[14,15] The use of an additional precursor introduces complexity, it can make it hard to control the nitrogen content, and the deposited film can change to TiN at high temperature.[16,17] Recently, plasma assisted atomic layer deposition (PAALD) was used for doping due to advantages such as higher reactivity, low deposition temperature,[18] and the possibility to control the chemical composition.[17] However, these efforts resulted in low nitrogen contents or required complex techniques or relatively long deposition times to obtain high nitrogen contents. Zhipeng *et al.*[19] deposited N-doped TiO_2 by PAALD with $TiCl_4$, H_2O, and N_2 plasma gas, achieving a doping level of 1 at. % of nitrogen. Deng *et al.*[20] achieved a nitrogen content of 9.4 at. % by alternating thermal ALD of TiO_2 and PAALD of TiN, but the use of alternating deposition methods required a longer deposition time. Zhang *et al.*[17] deposited $TiO_{2-x}N_x$ ultrathin films by varying the background gas (O_2 or N_2) during the Ti precursor exposure with a N_2/H_2-fed inductively coupled plasma (ICP). They achieved a significant nitrogen content of 13 at. %, as measured at the surface of the film, and up to 22 at. % in the bulk of the film by injecting N_2 gas for 4 s through the ICP dosing line during the Ti precursor exposure. Despite using a procedure without any oxygen precursor, the substitutional doping in their films was limited to 50%. Additionally, their approach used a long (15 s) H_2/N_2 plasma exposure time to achieve these nitrogen contents, which limits the film growth rate (up to 30 s required per cycle). Their approach is detailed schematically in Fig. 1. The PAALD cycle time is the sum of the Ti precursor dosing time, the Ti purge time, the reactant (O_2/N_2) dose time, and the reactant plasma purge time. Thus, using more reactants and longer exposure times leads to increased purge times and increased cycle times, resulting in slow film growth rates. Furthermore, some of the previous reports of N-doped TiO_2 by PAALD used $TiCl_4$ as the precursor,[19] which is undesirable due to resulting chlorine contamination. Because chlorine and oxygen have different ionic radii, chlorine impurities result in undesirable chemical properties.[21] Achieving N-doped TiO_2 with minimal contamination/

a)Electronic mail: kevin.musselman@uwaterloo.ca

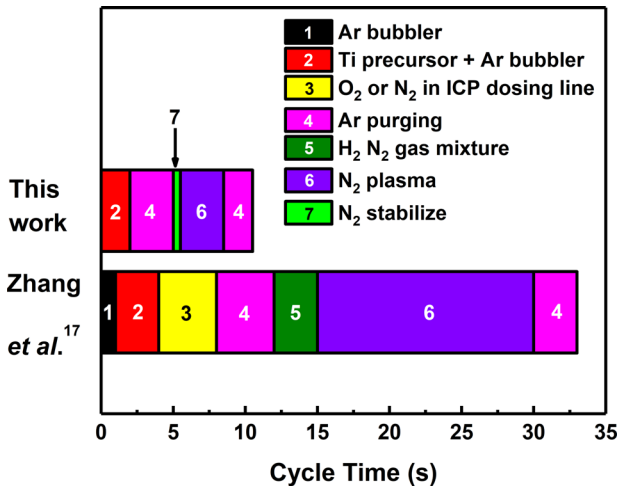

FIG. 1. (Color online) Flow chart of the PAALD cycle developed in this work and the cycle reported in previous work. Procedures that produced the highest nitrogen contents are shown.

impurities via faster depositions employing fewer precursors is challenging.

In this work, a simple and fast approach for PAALD of N-doped TiO_2 with a high nitrogen content and substitutional doping is designed and studied. Doping TiO_2 with nitrogen requires high energy because breaking of Ti–O bonds by nitrogen atoms is not thermodynamically favored.[20] Therefore, even when the nitrogen plasma flow was increased in PAALD previously, the nitrogen concentration in TiO_2 was low.[19] We use no O_2 precursor sources and a pure nitrogen plasma (unlike the mixed H_2/N_2 plasma used by Zhang *et al.*[17]) in the approach presented here so that the formation of Ti–O bonds is inhibited and nitrogen is more likely to react with Ti. Residual water vapor in the PAALD chamber was an oxygen source in a pressure range of 1.3×10^{-4} to 1.3×10^{-5} Pa, and thus, titanium isopropoxide was selected as the titanium precursor because it is highly reactive with water vapor. Even though there is very little water vapor in the chamber as compared to nitrogen, its affinity for the Ti precursor is much greater, which is expected to ensure the formation of N-doped TiO_2 in this arrangement, rather than TiN. However, by limiting the quantity of oxygen present and using a pure N_2 plasma, it is expected that nitrogen incorporation into the films will be enhanced and result in more substitutional doping of TiO_2.

II. EXPERIMENT

A. PAALD of N-doped TiO_2

Nitrogen-doped TiO_2 was deposited on silicon wafers (100 orientation) that were 2 in. in diameter and 13 to 17 thousandths of an inch (330 to 432 μm) thick, as identified by the manufacturer (Silicon Quest International), and glass substrates that were 25.4 ± 0.2 mm in diameter and 1.6 ± 0.2 mm thick. The depositions on the silicon and glass substrates were performed simultaneously in order to avoid any change in the deposition conditions. The films were deposited at 250 °C using an Oxford-FlexALTM system with a base pressure below 1.33×10^{-4} Pa. The moderate deposition temperature of 250 °C was selected to prevent the formation of TiN rather than TiO_2. The system utilized an ICP source for remote plasma operation. The diameter of the ICP tube was 80 mm, and the load lock of the system was pumped to below 1.33×10^{-3} Pa. The vacuum chamber was first purged with Ar for 3 min to stabilize the chamber pressure and temperature. Figure 1 illustrates the N-doped TiO_2 procedure used in this work, along with that of Zhang *et al.*[17] TIIP bubbled with argon was used to dose the substrate for 2 s at a pressure of 10.6 Pa, and then, the precursor line was purged with Ar for 3 s at a pressure of 2 Pa. For some depositions, a flow of O_2 was then stabilized for 500 ms before generating a plasma by radio frequency (RF) with a power of 300 W at a pressure of 2 Pa. Selected substrates were exposed to the O_2 plasma for 3 s and then purged with Ar for 2 s at a pressure of 10.6 Pa. The N_2 plasma flow was stabilized for 500 ms, and a RF plasma was generated with a power of 300 W. The substrates were exposed at a pressure of 2 Pa for different durations, followed by Ar purging for 2 s at a pressure of 10.6 Pa.

The O_2 and N_2 gas feeds, plasma exposure times, and number of PAALD cycles for different procedures tested are summarized in Table I. Notably, all procedures except the TiO_2 procedure and the first doping procedure did not employ the oxygen plasma such that the only sources of oxygen were the TIIP and residual water vapor in the vacuum chamber.

B. Characterization

UV-Vis spectroscopy (UV-2501 PC) with a wavelength range of 190–1100 nm, a resolution of 0.1 nm, a wavelength accuracy of ± 0.3 nm, and a precision of ± 0.002 abs was applied to measure the transmittance T and reflectance R of the films, as shown in Fig. S1 in the supplementary material.[42] The extinction coefficient k was calculated from the following relation:[22,23]

$$k = -\ln\left[T/(1-R)\right]\left[\lambda/4\pi d\right]. \quad (1)$$

In Eq. (1), λ is the wavelength and d is the film thickness. The absorption coefficient α was then calculated using the extinction coefficient k,

$$\alpha = [4\pi k/\lambda], \quad (2)$$

and the bandgaps of the films were determined using

TABLE I. Process procedures for PAALD films.

	Gas feed (sccm)				
Procedure	O_2	N_2	Plasma time (s)	No. of cycles	Base pressure
1	10	50	3	600	1.33×10^{-4} Pa
2	0	50	1	600	
3	0	50	3	600	
4	0	50	5	600	
5	0	50	7	600	
TiO_2	60	0	3	600	

$$\alpha hv = B[hv - E_g]^r, \quad (3)$$

where B is a constant, hv is the photon energy, E_g is the bandgap of the material, and $r = 2$ for an indirect bandgap, as reported previously.[24] The bandgaps of the films were calculated from Tauc plots[25] by plotting $(\alpha hv)^{1/2}$ versus the photon energy hv, where the tangent of the curve gives the bandgap of the film.

A Woollam M-2000 DI ellipsometer was used to measure the thickness of the films deposited on glass substrates for use in the bandgap calculations. Ellipsometry was also performed to measure the refractive indices of the films deposited on silicon wafers, where the deposited films were modeled using the Cauchy formula.

X-ray photo electron spectroscopy (XPS) (VG Scientific ESCALAB 250) was performed on the surface of the films using Al Kα x-rays. The spectra were calibrated using the C1s peak at 284.6 eV. XPS was performed using silicon substrates rather than glass to obtain more reliable results.

III. RESULTS AND DISCUSSION

The absorption coefficients calculated from the UV-vis transmittance and reflectance measurements are shown in Fig. 2(a). A similar absorption edge is observed at approximately 350 nm for the films deposited using the TiO_2 procedure and procedure 1 (3s O_2 and N_2 plasmas). A shift of the absorption edges to 450 nm for the second procedure (1s N_2 plasma), 520 nm for the third procedure (3s N_2 plasma), and 500 nm for the fourth and fifth procedures (5s and 7s N_2 plasmas) indicates the successful incorporation of nitrogen in all cases. Figure 2(b) shows the bandgaps identified using Tauc plots. The narrowing of the bandgap from 3.1 eV for TiO_2 to 1.9 eV for the films deposited using the third procedure (3s N_2 plasma) is consistent with previous reports[20] that showed narrowing of the bandgap to 1.91 eV.

The chemical composition and bonds between elements were characterized by XPS. Table II compares the XPS peak positions (Ti $2p^{3/2}$, Ti $2p^{1/2}$, N1s, and O1s) observed in this work with those of TiN, TiNO, and N-doped TiO_2 reported previously in the literature. It is seen that the peak positions measured here are consistent with N-doped TiO_2, rather than TiN or TiNO. To further confirm that N-doped TiO_2 was deposited, the refractive indices of the films were measured by ellipsometry. Figure S2 in the supplementary material shows that the refractive index values at 632.8 nm (start of the red part of the visible spectrum) were in the range of 2.4 to 2.9, consistent with previous reports that showed 2.4 (Ref. 23) and 2.9 (Ref. 26) for TiO_2. The slight variation in the refractive index likely comes from composition changes in the N-doped TiO_2 films made using different procedures. In contrast, the refractive index of TiN is typically reported to be approximately 1.7.[22]

Figure 3 shows the Ti 2p XPS spectra of the films. Ti $2p_{3/2}$ and Ti $2p_{1/2}$ peaks are located at 458 eV and 464 eV, respectively, for the TiO_2 procedure in Fig. 3(a), and are attributed to TiO_2 (Ti^{4+}). For procedure 1 (3s O_2 and N_2 plasmas), the same Ti^{4+} peaks are observed in Fig. 3(b). When a N_2 plasma is used without O_2 gas, as in procedures 2–5, Ti 2p peaks appear at 457 and 463 eV [as shown in Figs. 3(c)–3(f)], which are attributed to Ti_2O_3 (Ti^{3+}).[36] The appearance of the Ti^{3+} peaks coincides with the shifting of the bandgap in Fig. 2, suggesting that the Ti^{3+} peaks appear when the nitrogen content is increased in the films. While small peaks corresponding to Ti^{4+} and TiO also appear in Figs. 3(c)–3(f) for procedures 2–5 that only used a N_2 plasma,[22] the Ti^{3+} peaks clearly dominate. This change from Ti^{4+} to Ti^{3+} is consistent with the film composition information obtained by XPS and reported in Table III. While surface contamination is expected to influence the measured composition values somewhat, a clear reduction in the O/Ti ratio from approximately 2.3 for the procedures that employed an O_2 plasma (procedures 1 and TiO_2) to approximately 1.8–2 for procedures 2–5 that only used a N_2 plasma is seen in Table III. This coincides with the introduction of nitrogen concentrations of 14 to 23 at. %, which are also reported in Table III.

Figure 4 shows that N1s XPS peaks are present for all procedures that employed the N_2 plasma, confirming that nitrogen is incorporated successfully into the TiO_2 lattice. It is generally agreed that N1s XPS peaks in the ranges of 396

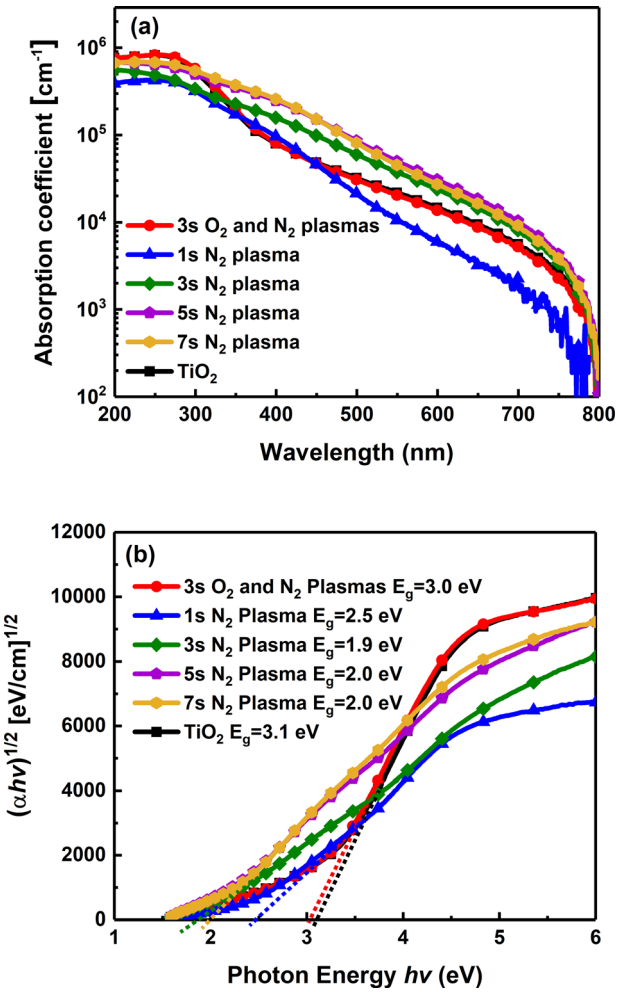

FIG. 2. (Color online) (a) Absorption coefficient and (b) Tauc plots of TiO_2 and N-doped TiO_2 films.

TABLE II. Literature data on the XPS binding energies (eV) of Ti 2p, N1s, and O1s (Ref. 27).

Films	Ti $2p^{3/2}$	Ti $2p^{1/2}$	N1s	O1s
TiN	455.2 (Ref. 28)	461 (Ref. 20)	396 (Ref. 29), 397 (Ref. 30)	Ti-O 531 (Ref. 28)
TiNO	455.2 (Ref. 31)	461 (Ref. 31)	397 (Ref. 30)	Ti-O 531 (Ref. 28)
N-doped TiO_2	456–459 (Ref. 29)	463–465 (Ref. 29)	Ti-N (396) (Refs. 33 and 34) O-Ti-N (398) (Ref. 34) Ti-O-N (400) (Ref. 35)	Ti-O 529.7 (Ref. 28) OH 531 (Ref. 20)
	459.1 (Ref. 32)			
This work	Procedure 1: 458.5	464	Ti-N 396 Ti-O-N 400	Ti-O 529.7 OH 531
	Procedure 2: 457	464	Ti-N 396 O-Ti-N 398 Ti-O-N 400	Ti-O 529.4 OH 530.1
	Procedure 3: 457	463	Ti-N 396 O-Ti-N 398	Ti-O 529.7 OH 530
	Procedure 4: 457.4	462.5	Ti-N 396 O-Ti-N 398 Ti-O-N 400	Ti-O 529.4 OH 530.1
	Procedure 5: 457	463	Ti-N 396 O-Ti-N 398 Ti-O-N 400	Ti-O 529.3 OH 530.1
	TiO_2: 458.5	464	—	Ti-O 529.6 OH 530

to 398 and 399 to 402 eV correspond to substitutional nitrogen and interstitial nitrogen (or chemisorbed species), respectively.[37] Figure 4(a) shows a weak interstitial N peak (Ti-O-N) at 400 eV and a weak peak at 402 eV for the TiO_2 procedure, which are attributed to chemisorbed N_2 (Refs. 15 and 33). Procedure 1, which employed 3s O_2 and N_2 plasmas, shows a small interstitial peak (Ti-O-N) at approximately 400 eV in Fig. 4(b), as well as a weak substitutional peak at 396 eV (labeled "Ti-N"). The N1s XPS spectra of the films produced using a N_2 plasma only (procedures 2–5) are shown in Figs. 4(c)–4(f) and demonstrate substitutional peaks at approximately 396 and 398 eV, as well as interstitial nitrogen peaks at approximately 400 eV. It was noted by Viswanathan and Krishanmurthy that if nitrogen assumes anionic substitutional states in TiO_2, a binding energy of around 394 eV is expected, whereas 400 eV would be expected for cationic states.[37] They explained that if the Ti-N bond were to assume covalent character, the binding energy could vary with the extent of loading and possibly account for the variation in binding energy values reported in the literature, such as the two peaks at 396 and 398 eV observed in this work. Sathish *et al.*, for example, attributed a substitutional peak at 398 eV to anionic N^- in O-Ti-N linkages.[29] Thus, the distinction between these two peaks is

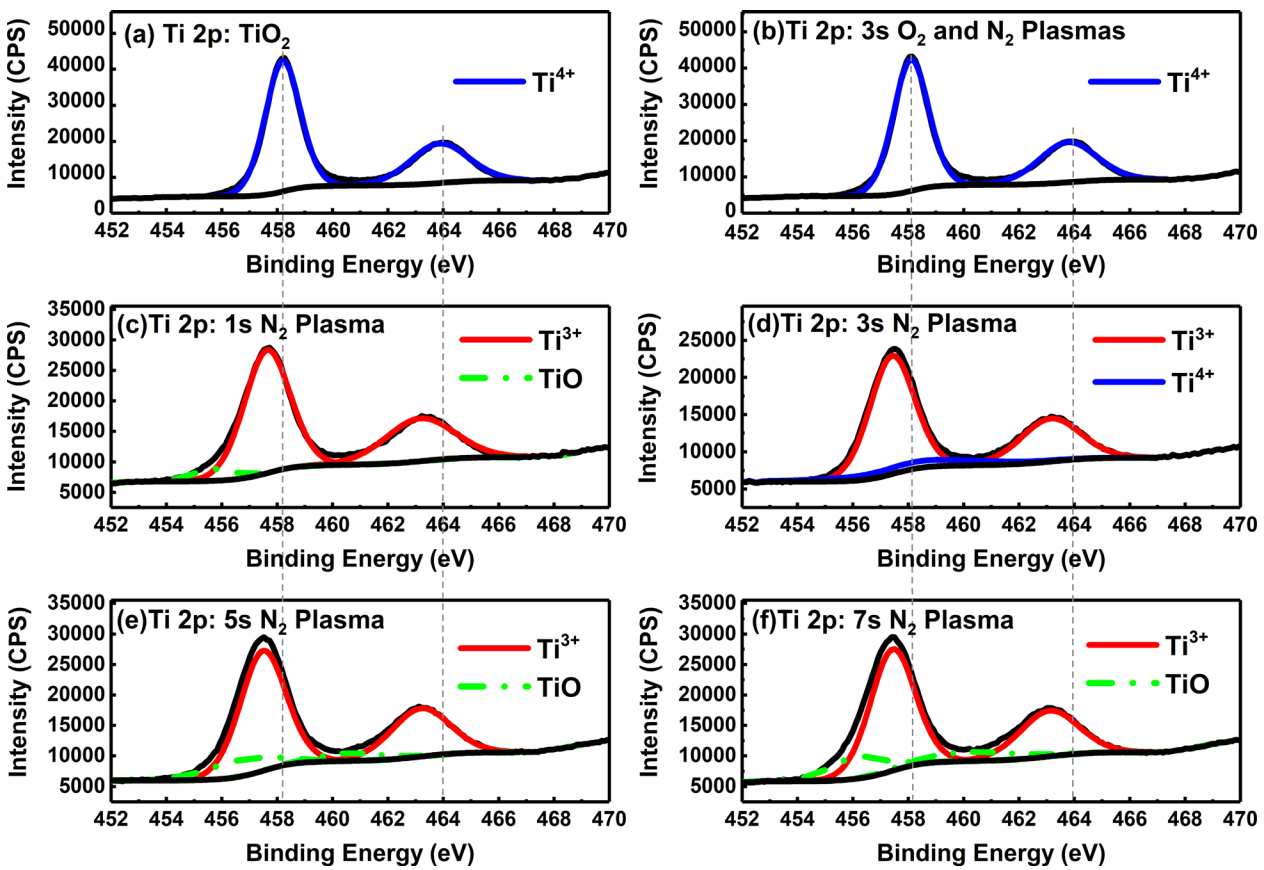

FIG. 3. (Color online) Ti 2p XPS spectra of TiO_2 and N-doped TiO_2 films: (a) TiO_2, (b) 3s O_2/N_2 plasmas, (c) 1s N_2 plasma, (d) 3s N_2 plasma, (e) 5s N_2 plasma, and (f) 7s N_2 plasma. CPS, counts per second.

TABLE III. Film compositions of PAALD samples.

Procedure	Film compositions (at. %)						Fraction (%)[a]	
	Ti	O	N	C	N/Ti	O/Ti	N_{inte}	N_{sub}
1	23.6 ± 0.2	56.0 ± 0.4	0.4 ± 0.2	20.0 ± 0.5	0.02	2.37	88	12
2	17.4 ± 0.4	36.0 ± 0.3	14.4 ± 0.3	32.0 ± 0.3	0.82	2.06	17	83
3	13.1 ± 1.0	26.0 ± 0.1	23.0 ± 0.5	37.8 ± 0.4	1.75	1.98	0	100
4	19.3 ± 0.3	35.0 ± 0.3	19.0 ± 0.4	26.8 ± 0.8	0.98	1.81	8	92
5	19.8 ± 0.4	36.0 ± 0.5	15.7 ± 0.5	27.8 ± 0.5	0.79	1.81	7	93
TiO_2	24.0 ± 0.6	55.0 ± 0.3	0	21.0 ± 0.7	0	2.30	–	–

[a]Calculated based on the area of the $N_{interstitial}$ and $N_{substitutional}$ peaks, compared to the total area of the N1s peaks.

unclear and warrants further study; however, within the scope of this work, it is sufficient to ascribe these two peaks to substitutional nitrogen, in agreement with the existing literature. The relative intensities of these two substitutional peaks have been reported to be different for different fabrication processes.[37] The substitutional peak at 398 eV, which is attributed to the N^- anion, is expected to be responsible for changing the Ti^{4+} valence state.[37] This agrees with our measurements, as it is seen that procedure 3 (3s N_2 plasma) had the most dominant 398 eV peak [Fig. 4(d)] and resulted in Ti 2p XPS spectra consisting almost exclusively of a Ti^{3+} signal [Fig. 3(d)]. Only the substitutional nitrogen peaks at 396 and 398 eV are present for the 3s N_2 plasma exposure (procedure 3) in Fig. 4(d), whereas an interstitial (Ti-O-N) peak is also present for the 1s, 5s, and 7s N_2 plasma exposures in Figs. 4(c), 4(e), and 4(f). The fraction of the N1s signal attributable to interstitial and substitutional nitrogen is calculated based on the area under the corresponding XPS peaks and reported in Table III, with 100% substitutional doping observed for the 3s N_2 plasma (procedure 3).

The nitrogen concentration and N/Ti ratio reported in Table III display similar trends as the ratio of substitutional to interstitial doping. Both increase to their maximum values when the N_2 plasma time is increased from 1 s (procedure 2)

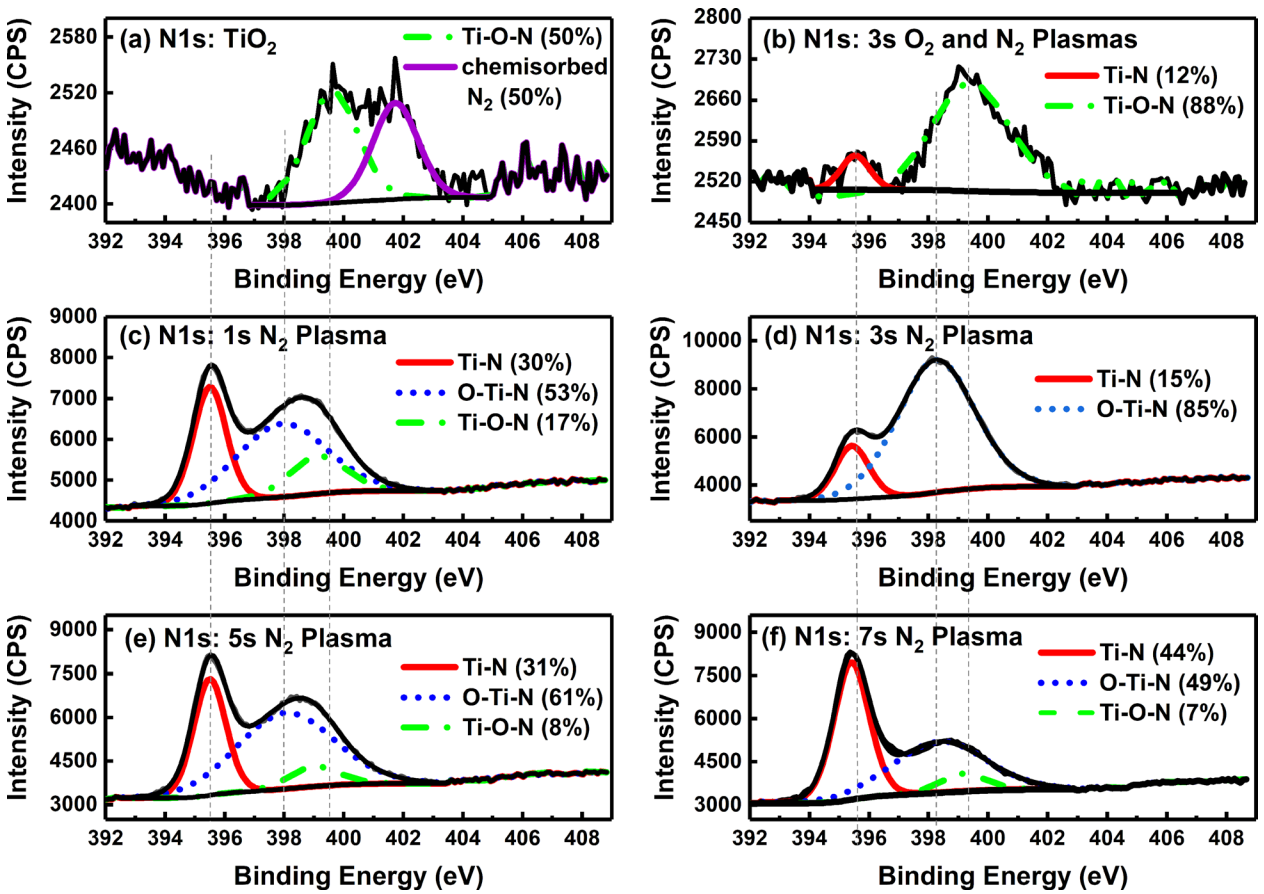

FIG. 4. (Color online) N1s XPS spectra of TiO_2 and N-doped TiO_2 films: (a) TiO_2, (b) 3s O_2/N_2 plasmas, (c) 1s N_2 plasma, (d) 3s N_2 plasma, (e) 5s N_2 plasma, and (f) 7s N_2 plasma.

to 3 s (procedure 3) and then decrease for longer plasma times (procedures 4 and 5). For example, the nitrogen content increases from 14.4 ± 0.3 at. % to 23.2 ± 0.5 at. % when the N_2 plasma exposure is increased from 1 s to 3 s and then decreases to 19.0 ± 0.4 at. % and 15.7 ± 0.5 at. % for longer N_2 plasma exposure times of 5 s and 7 s. These results suggest that approximately 3 s is required for the N_2 plasma to react with the monolayer of the Ti precursor. The thicknesses of the samples were measured by ellipsometry to be 23.1 ± 0.1 nm for the 3s O_2 and N_2 plasmas (procedure 1), only 11.7 ± 0.2 nm for the 1s N_2 plasma (procedure 2), 22.3 ± 0.1 nm for the 3s N_2 plasma (procedure 3), 18.5 ± 0.4 nm for the 5s N_2 plasma (procedure 4), 18.5 ± 0.1 nm for the 7s N_2 plasma (procedure 5), and 26 ± 0.2 nm for the TiO_2 procedure. The 11.7 nm thickness obtained using 600 cycles of procedure 1 confirms that 1s of N_2 plasma exposure is insufficient. The decreased nitrogen concentration, decreased N/Ti ratio, and reduced fraction of substitutional doping observed for the 5s and 7s N_2 plasma exposures, compared to the 3 s exposure, suggest that for N_2 plasma exposure times longer than 3 s, formed Ti–N bonds may be broken by subsequent thermodynamically favored titanium-oxygen reactions. Figure 5 plots the fraction of substitutional and interstitial nitrogen as a function of N_2 plasma exposure time. It appears that for extended plasma exposures, reactions between the titanium precursor and residual water in the chamber may result in nitrogen atoms being moved from substitutional to interstitial positions, as oxygen atoms take their place, and then gradually expelled from the films altogether.

The location of nitrogen atoms in the TiO_2 lattice is important for catalyst performance[38] and can also influence the bandgap.[36] Figure 5 also plots the bandgap as a function of the N_2 plasma exposure. It is seen that the trend in the bandgap narrowing is similar to the increase in substitutional nitrogen doping. Notably, the 100% substitutional doping achieved using procedure 3 (3s N_2 plasma) is higher than that reported previously for PAALD.[17] The fraction of interstitial doping can be increased by increasing the N_2 plasma exposure time or introducing an O_2 plasma.

The nitrogen concentration of 23.2 ± 0.5 at. % that is observed for the film deposited using 3s N_2 plasma exposures is higher than that reported previously for PAALD of N-doped TiO_2.[17,19,20] Furthermore, procedure 3 uses a N_2 plasma exposure time that is five times shorter than that used by Zhang *et al.*[17] to produce a nitrogen content of 13 at.% at the film surface (22 at. % in the bulk). The resulting cycle time (10.5 s/cycle) is three times shorter than that used by Zhang *et al.*[17] as shown in Fig. 1. This procedure also demonstrates the ability of a N_2 plasma environment to dope TiO_2 more effectively, particularly in a substitutional manner, than some plasma environments that make use of NH_3.[39] The carbon contamination observed in Table III is consistent with previous reports that used TIIP and oxygen plasma.[40] It may be due to incomplete reaction between the TIIP and the nitrogen plasma, which could leave significant amounts of unreacted precursors. Zhang *et al.*[17] also observed a significant amount of carbon (33 at. %), similar to the amount observed in this work, due to the incomplete reaction of TDMAT with nitrogen. Air contamination resulting from transporting the samples to the XPS equipment is also expected. Finally, Fig. 6 shows the O1s peaks for the samples made using the TiO_2 procedure and

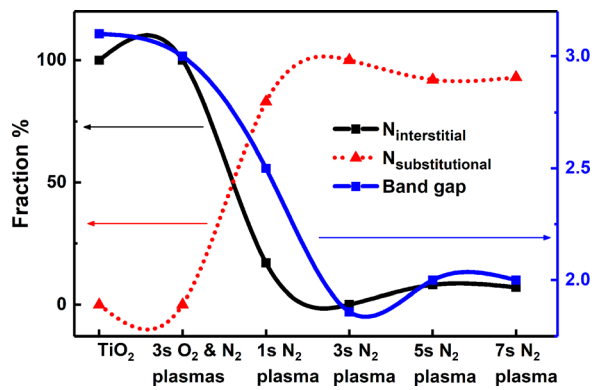

FIG. 5. (Color online) $N_{interstitial}$ and $N_{substitutional}$ peak intensities with the bandgap.

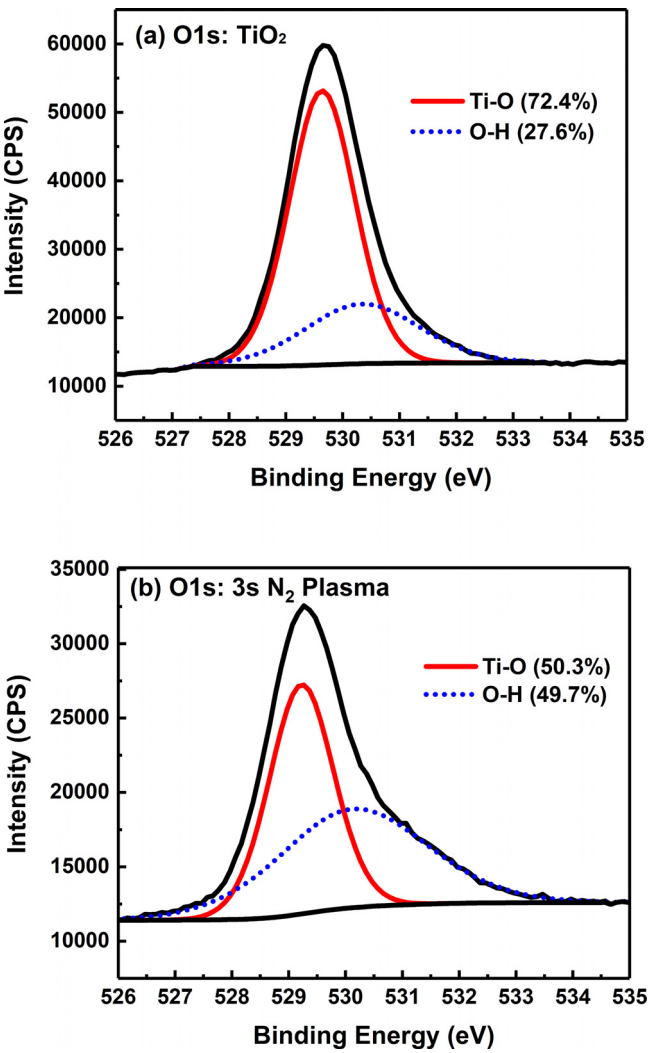

FIG. 6. (Color online) O1s XPS spectra of (a) TiO_2 and (b) N-doped TiO_2 made using 3s N_2 plasma exposures.

procedure 3 (3s N_2 plasma). The very high affinity of titanium for oxygen[41] is expected to result in the Ti precursor atoms accommodating available oxygen in the chamber. By using a procedure with no O_2 plasma (procedure 3), the Ti-O bond intensity was decreased, as shown in Fig. 6(b). The O-H signal is attributed to hydroxyl groups on the surface of the films. It is expected that by limiting the formation of Ti–O bonds, it was possible to incorporate more nitrogen atoms into the films (substitutional and interstitial) via exposure to the nitrogen plasma.

IV. SUMMARY AND CONCLUSIONS

A simple and fast PAALD technique to dope TiO_2 with nitrogen was demonstrated. UV-visible measurements showed narrowing of the bandgap from 3.1 to 1.9 eV. XPS characterization demonstrated a higher nitrogen content (23 ± 0.5 at. %) than reported previously for nitrogen doping with PAALD although carbon and oxygen contamination influenced this measured value. This method required no O_2 precursor, high temperatures, or postchemical treatments to enhance the nitrogen content in the TiO_2 films. It required only one reactant plasma with a short exposure time (1 to 7 s). Furthermore, it was demonstrated that the nitrogen doping could be tailored from 100% substitutional to almost entirely interstitial doping by varying the plasma exposure time.

ACKNOWLEDGMENTS

A.A. would like to acknowledge Prince Sattam bin Abdul Aziz University, Alkharj, Saudi Arabia, for financial support. The University of Waterloo's Quantum NanoFab was used for device fabrication. The Quantum NanoFab acknowledges support from the Canada Foundation for Innovation, the Ontario Ministry of Research and Innovation, Industry, Canada, and Mike and Ophelia Lazaradis.

[1]J. Bai and B. Zhou, Chem. Rev. **114**, 10131 (2014).
[2]M. Grätzel, J. Sol-Gel Sci. Technol. **22**, 7 (2001).
[3]I. P. Parkin and R. G. Palgrave, J. Mater. Chem. **15**, 1689 (2005).
[4]A. Kafizas and I. P. Parkin, J. Mater. Chem. **20**, 2157 (2010).
[5]K. Vasu, M. B. Sreedhara, J. Ghatak, and C. Rao, ACS Appl. Mater. Interfaces **8**, 7897 (2016).
[6]B. Liu, L. Wen, and X. Zhao, Sol. Energy Mater. Sol. Cells **92**, 1 (2008).
[7]Y. Suda, H. Kawasaki, T. Ueda, and T. Ohshima, Thin Solid Films **453**, 162 (2004).
[8]V. Pore, A. Rahtu, M. Leskelä, M. Ritala, T. Sajavaara, and J. Keinonen, Chem. Vap. Deposition **10**, 143 (2004).
[9]L. Aarik, T. Arroval, R. Rammula, H. Mändar, V. Sammelselg, and J. Aarik, Thin Solid Films **542**, 100 (2013).
[10]V. Pore, T. Kivelä, M. Ritala, and M. Leskelä, Dalton Trans. **0**, 6467 (2008).
[11]J. Löckinger, S. Nishiwaki, T. P. Weiss, B. Bissig, Y. E. Romanyuk, S. Buecheler, and A. N. Tiwari, Sol. Energy Mater. Sol. Cells **174**, 397 (2018).
[12]A. Sasinska, D. Bialuschewski, M. M. Islam, T. Singh, M. Deo, and S. Mathur, J. Phys. Chem. C **121**, 15538 (2017).
[13]Y. Zhang, C. Guerra-Nuñez, I. Utke, J. Michler, P. Agrawal, M. D. Rossell, and R. Erni, Chem. Mater. **29**, 2232 (2017).
[14]V. Pore, M. Heikkilä, M. Ritala, M. Leskelä, and S. Areva, J. Photochem. Photobiol., A **177**, 68 (2006).
[15]H. Cheng, W. Lee, C. Hsu, M. Hon, and C. Huang, Electrochem. Solid-State Lett. **11**, 81 (2008).
[16]Y. Zhang, Q. Ma, L. Gao, and E. J. Hensen, Appl. Surf. Sci. **282**, 174 (2013).
[17]Y. Zhang, M. Creatore, Q. Ma, A. El Boukili, L. Gao, M. A. Verheijen, and E. J. Hensen, Appl. Surf. Sci. **330**, 476 (2015).
[18]H. B. Profijt, S. E. Potts, M. Van de Sanden, and W. Kessels, J. Vac. Sci. Technol., A **29**, 050801 (2011).
[19]R. Zhipeng, W. Jun, L. Chaobo, C. Bo, L. Jian, H. Chengqiang, and X. Yang, Plasma Sci. Technol. **16**, 239 (2014).
[20]S. Deng *et al.*, J. Vac. Sci. Technol., A **32**, 01123 (2014).
[21]A. Goossens, E. Maloney, and J. Schoonman, Chem. Vap. Deposition **4**, 109 (1998).
[22]J. Rodrıguez, M. Gomez, J. Ederth, G. A. Niklasson, and C. G. Granqvist, Thin Solid Films **365**, 119 (2000).
[23]P. Wu, C. Ma, and J. K. Shang, Appl. Phys. A **81**, 1411 (2005).
[24]R. López and R. Gómez, J. Sol-Gel Sci. Technol. **61**, 1 (2012).
[25]J. Tauc, R. Grigorovici, and A. Vancu, Phys. Status Solidi B **15**, 627 (1966).
[26]J. Barth, R. L. Johnson, and M. Cardona, *Handbook of Optical Constants of Solids II*, edited by E. Palik (Academic, New York, 1991).
[27]C. Chen, H. Bai, and C. Chang, J. Phys. Chem. C **111**, 15228 (2007).
[28]N. C. Saha and H. G. Tompkins, J. Appl. Phys. **72**, 3072 (1992).
[29]L. Miao, S. Tanemura, H. Watanabe, Y. Mori, K. Kaneko, and S. Toh, J. Cryst. Growth **260**, 118 (2004).
[30]G. A. Battiston, R. Gerbasi, A. Gregori, M. Porchia, S. Cattarin, and G. A. Rizzi, Thin Solid Films **371**, 126 (2000).
[31]J. Guillot, A. Jouaiti, L. Imhoff, B. Domenichini, O. Heintz, S. Zerkout, A. Mosser, and S. Bourgeois, Surf. Interface Anal. **33**, 577 (2002).
[32]M. Maeda and T. Watanabe, J. Electrochem. Soc **153**, 186 (2006).
[33]R. Asahi, T. Morikawa, T. Ohwaki, K. Aoki, and Y. Taga, Science **293**, 269 (2001).
[34]M. Sathish, B. Viswanathan, R. P. Viswanath, and C. S. Gopinath, Chem. Mater. **17**, 6349 (2005).
[35]J. Wang, D. N. Tafen, J. P. Lewis, Z. Hong, A. Manivannan, M. Zhi, M. Li, and N. Wu, J. Am. Chem. Soc. **131**, 12290 (2009).
[36]J. Lynch, C. Giannini, J. K. Cooper, A. Loiudice, I. D. Sharp, and R. Buonsanti, J. Phys. Chem. C **119**, 7443 (2015).
[37]B. Viswanathan and K. R. Krishanmurthy, Int. J. Photoenergy **2012**, 269654 (2012).
[38]S. A. Ansari, M. M. Khan, M. O. Ansari, and M. H. Cho, New J. Chem. **40**, 3000 (2016).
[39]D. J. Pulsipher, I. T. Martin, and E. R. Fisher, ACS Appl. Mater. Interfaces **2**, 1743 (2010).
[40]J. Musschoot, "Advantages and challenges of plasma enhanced atomic layer deposition," Ph.D. thesis (University Gent, 2011).
[41]*Titanium: A Technical Guide*, edited by M. J. Donachie (ASM International, US, 2000).
[42]See supplementary material at https://doi.org/10.1116/1.5019170 for reflectance, transmittance, and refractive index measurements for the films.